ABUAD Journal of Engineering Research and Development (AJERD)
ISSN (online): 2645-2685; ISSN (print): 2756-6811

Volume 8, Issue 1, 88-103

Biosorption of Chromium and Nickel from Industrial Oil Mill Wastewater Using Groundnut Pod Waste Activated Carbon

Nanret Liba YACEH, Michael Sunday OLAKUNLE, Nehemiah Samuel MAINA

Department of Chemical Engineering, Ahmadu Bello University Zaria, Kaduna State, Nigeria
libananret@gmail.com/msmolakunle@gmail.com/nsmaina@yahoo.com

Corresponding Author: libananret@gmail.com, +2347030076778
Date Submitted: 25/06/2024
Date Accepted: 8/12/2024
Date Published: 3/02/2025

Abstract: *Groundnut shell activated carbon was developed and characterized by chemical activation using phosphoric acid (H_3PO_4) for the uptake of Cr and Ni in a batch biosorption process. The purpose of this study was to reduce the spread of heavy metals in industrial oil mill wastewater. In this study characterization of activated carbon using, surface chemistry (FTI-IR), surface area (BET), surface morphology, and elemental identification (SEM/EDX) were all carried out, and the BET surface area was 689.41 m^2/g for groundnut shell activated carbon. This study was also executed to determine the optimum biosorption efficiency parameters for Cr and Ni removal using Response Surface Methodology (RSM) to obtain maximum biosorption efficiency. The factors considered were temperature (25-55^oC), adsorbent dosage (0.2-3 g) and contact time (1-2 hrs). Biosorption efficiency was the response. ANOVA analysis was carried out to analyse the most effective factor in experimental design response. The optimum conditions for removal of Cr and Ni were adsorbent dosage 0.40 g, contact time 1.1 hr and temperature 42.02 ^oC, which shows the maximum biosorption efficiency of 97.1% for Cr removal and 94.8% for Ni removal. Isotherm models analyses showed that the biosorption process was best fitted to Langmuir model and was physical. Results of the kinetic studies and thermodynamic parameters revealed that the biosorption process followed a pseudo-second-order, endothermic, and spontaneous in nature*.

Keywords: *Groundnut Shell Activated Carbon, Heavy Metals, Characterization, Biosorption Efficiency, Response Surface Methodology*

1. INTRODUCTION

Industrialization has led to introduction of pollutants such as pesticides, herbicides, fertilizers, household wastes, industrial wastes, volatile organic compounds, and heavy metals into water bodies and the environment. Water plays major role in the world economy. The Earth's surface is majorly covered by water about (71%), but fresh water forms a very small fraction of the total about (3%) [1]. Water suitable for human use is gotten from the fresh water bodies. Agriculture takes about 70% of the fresh water. Fresh water is in short supply in many areas and its insufficiency is a major environmental concern [2].

In some developing nations, about 90% of wastewater goes untreated into fresh water bodies making it unsuitable for human use as some of this wastewater contains toxic organic compounds and heavy metals, which affects the health of human population causing diseases such as diarrhea, typhoid fever, skin irritation, liver, kidney and heart diseases e.t.c. [1]. The interest to safeguard fresh water bodies for a healthy population is on the increase [3].

Agricultural waste residue from the growing and processing of raw agricultural products has become a major problem of environmental pollution as it has become a solid waste management problem. The need to converting some of this agricultural waste into useful product such as bio-sorbent for wastewater treatment is on the rise, there by solving solid waste management challenge. Groundnut shell is an agricultural waste that is used for livestock feed and has been used as biosorbent for wastewater treatment [4].

Researchers have also set up the effectiveness of activated carbon from agricultural wastes as one of the best biosorbents for heavy metal removal from industrial wastewater. Activated carbon is very porous with a large surface area and commonly produced from organic materials such as groundnut shells, palm kernel, coconut shells, corncob, wood chips, sawdust and seedpods [5]. Activated carbon biosorption is a process that is largely utilized for removal of waste from effluents. Biosorption depends on the large surface area of the biosorbent, with its micro-porous structure, resulting in high biosorption capacity. It is normally easy to execute and gives high biosorption efficiency [6]. Activated carbon from agricultural waste materials promises a good outlook for future in link with their usual availability, reusability, and profitability [7].

Previous studies have looked into the effect of different biosorption parameters, such as temperature, time, and adsorbent dosage on the biosorption of heavy metals from industrial wastewater. However, these studies have reported high biosorbent dosage and long contact time to achieve a substantial rate of biosorption [8, 9, 10].

This work is aimed at preparing activated carbon as a biosorbent from groundnut shell activated carbon through chemical activation, using phosphoric acid (H_3PO_4) for chromium and nickel sorption from an industrial oil mill wastewater through batch biosorption process.

Response Surface Methodology (RSM) is a compilation of numerical and statistical methods to make use of quantitative information from suitable approximation relationship and experimental design to analyse optimum operating conditions that are suitable for the modelling and analysis of engineering problem [11]. The Response Surface Methodology is getting popular among researchers for many applications; it is known to be promising optimization tools [12]. In this study, the Central Composite Design (CCD) of the RSM was used for modelling and optimization of the process data for the biosorption process.

2. MATERIALS AND METHOD

2.1 Materials

For this study, analytical grade phosphoric acid (H_3PO_4) 98% w/w purity, analytical reagent grade by BDH Chemicals was used for the experiment without additional purifications. The raw materials used were agricultural waste (groundnut shell obtained from Zaria) and industrial oil mill wastewater.

2.2 Method

2.2.1 Proximate analysis

Proximate analysis for groundnut shell was carried out to analyse, moisture content, ash content, volatile matter, and fixed carbon.

2.2.2 Groundnut shell activated carbon preparation

Groundnut shell was washed and sun dried till a fixed weight was achieved after which it was crushed and reduced in size using laboratory milling machine.

The crushed groundnut shell was poured into a crucible and put in a furnace set at 400°C for 30 min at 10°C/min heating rate in N_2. The furnace was turned off and the samples were left to cool at room temperature after carbonization.

For acid activation, groundnut shell carbon was impregnated with H_3PO_4 and the impregnation ratio between the groundnut shell carbon with H_3PO_4 was (gSample /gH_3PO_4) 1:1 g/g and it was left overnight at room temperature, following the method as described by [7].

The activated carbon (biosorbent) was washed with distilled water several times until a neutral pH of about 6.9–7 was attained, activated carbon was then left in the oven to dry at 80°C for 8 hours, and was reduced to a particle size of 125 µm and finally kept in an airtight container for use.

The operating conditions of carbonization temperature and impregnation ratio implemented in this study were modified from [7].

2.2.3 Proximate Analysis

i. **Moisture content** is identified by losses of weight at specific high temperature:

$$\%\ \text{Moisture} = \frac{\text{weight of sample + dish before drying – weight of sample + dish after drying}}{\text{weight of sample taken}} \times 100 \quad (1)$$

ii. **Ash content** is the residue remaining after combustion at a final temperature:

$$\%\ \text{Ash} = \frac{\text{weight of crucible + ash – weight of crucible}}{\text{weight of sample}} \times 100 \quad (2)$$

iii. **Volatile matter** is the portion of sample that is released as gasses or liquids during combustion**:**

$$\%\ \text{Moisture} = \frac{\text{weight of preheated sample – weight of sample after heating}}{\text{weight of precombustion sample}} \times 100 \quad (3)$$

iv. **Fixed carbon** is the difference between these parameters (moisture, volatiles and ash) it represents the amount of non-volatile carbon remaining in the sample after the volatile matter is expelled:

$$\%\ \text{Fixed carbon} = 100 - (\%\ \text{moisture content} + \%\ \text{ash content} + \%\ \text{volatile matter}) \quad (4)$$

2.2.4 Activated carbon percentage yield

During activated carbon preparation, the percentage yield is described as the final weight of activated carbon produced after carbonization, activation, washing and drying, then divided by initial weight of raw material, both on dry basis. Activated carbon percentage Yield was evaluated using Equation (5)

$$\%\ Yield = \frac{m}{m_o} \times 100 \quad (5)$$

Where m weight of final activated carbon (g) in dry form and m_o is the weight of raw material (g) in dry form

2.2.5 Characterization

The prepared biosorbent was examined through Brunauer-Emmett-Teller (BET) to determine the porosity and surface area. Scanning Electron Microscopy (SEM) was carried out to determine samples' surface morphology. Fourier transform infrared spectroscopy (FT-IR) was used to find out the surface chemistry, to identify the functional groups and covalent bonds vibration type present in the sample, the spectral data were compared to a reference. X-ray Fluorescence Spectrometer (XRF) and Atomic Absorption Spectroscopy (AAS) was used to find out the elemental composition, (for determination of initial concentration of metals in wastewater and final concentration of metals after biosorption).

2.2.6 Sorption studies

Batch studies were performed by charging 100 ml of the industrial oil mill wastewater into different containers (500 mL Erlenmeyer flask), and 0.2 – 3 g of groundnut shell activated carbon were carefully measured, then it was poured into each containers containing the wastewater at a constant pH 6.9.

The flasks were placed into a water-bath with a stirrer set at 160 rpm speed with a varrying temperatures set within the range of 25°C -55°C for a contact time between 1-2 hrs so that equilibrium could be attained. The entire process was executed based on data generation from Central Composite Design (CCD) of Response Surface Methodology (RSM), CCD design matrix is presented in Table 4. Before the attainment of equilibrium state, samples at separate experimental time intervals were taken and then filtered by the using a micropore filter membrane (45 µm) to establish the biosorbates remaining. The uptake of metal ions at equilibrium q, and biosorption efficiency R% were evaluated as in Equations (6) and (7)

$$q = \frac{(Ci-Cf)V}{m} \quad (6)$$

Where q is the metal uptake by the adsorbent (mg /g), C_i is the initial metal ion concentration in the solution (mg /L), C_f is the final metal ion concentration in the solution (mg /L), V is the volume of the working solutions (L), and m is mass of biosorbent used in biosorption process (g). Biosorption efficiency known as (R%) for the metal removal was calculated from Equation 7.

$$R\% = \frac{Ci-Cf}{Ci} \times 100 \quad (7)$$

Where R% is biosorption efficiency, C_i is initial metal ion concentration in the solution (mg /L), C_f is final metal ion concentration in the solution (mg /L) [13].

2.2.7 Adsorption isotherm studies

Adsorption isotherm represents the connection between the adsorbate in the surrounding phase and adsorbate absorbed on the surface of adsorbent at equilibrium and constant temperature. Adsorption is often designed by isotherms, which connect the relative concentrations of solute adsorbed to the solid (qe) and in solution which is the equilibrium concentration (Ce). Equilibrium data are usually examined with commonly used nonlinear isotherm models [14].

i. **Langmuir and Freundlich adsorption isotherm for Cr and Ni removal:** The Langmuir adsorption isotherm was applied to analyse the experimental data according to the non-linear equation represented by Equation (8).

$$q_e = \frac{q_m K_L C_e}{1+K_L C_e} \quad (8)$$

Where q_e is equilibrium biosorption capacity (mg/g); C_e is the metal ion concentration at equilibrium (mg/L); q_m is the maximum biosorption capacity (mg/g); and K_L is Langmuir constant (L/mg).

Furthermore, a dimensionless separation factor called equilibrium parameter R_L is also an essential characteristic of the Langmuir isotherm, which can be expressed as given in Equation (9).

$$R_L = \frac{1}{1+ K_L C_e} \quad (9)$$

Where K_L remains the Langmuir constant (L mg^{-1}) and Ce is the metal ion concentration at equilibrium (mg/L); the parameter R_L signifies the shape or type of isotherm as follows with value of $R_L>1$ is Unfavorable, $R_L=1$ is Linear, $0<R_L<1$ is Favorable, $R_L=0$ is Irreversible respectively.

The Freundlich adsorption isotherm model was also used to analyze the experimental data. The linear form of the model equation is given as Equation (10).

$$q_e = K_F C_e^{\frac{1}{n}} \quad (10)$$

Where q_e is the quantity of ions biosorbed per unit weight of biosorbent (mg/g). C_e is the equilibrium concentration of the biosorbate after biosorption has taken place (mg/L). K_F is Freundlich constant; and 1/n is biosorption intensity. K_F (L/g) is the Freundlich biosorption capacity, n = heterogeneity factor of biosorption sites (dimensionless); If a value for n = 1, the biosorption is linear, for n<1, the biosorption is chemisorption and n > 1, the biosorption is favorable physical process [15].

2.2.8 Kinetic study

The kinetic study of biosorption of chromium and copper was performed for a better understanding and comprehension of the efficiency of the biosorbents. Two kinetic models have been used to describe the biosorption kinetics of chromium and Nickel removal**,** the Lagergren pseudo first-order model and pseudo second-order.

The Lagergren equation express the biosorption rate in the solute-biosorbent systems and is largely used for the pseudo first-order kinetics which is usually given in the integrated form as;

$$\log(q_e - q_t) = \log q_e - \frac{k_1 t}{2.303} \quad (11)$$

Where qe and qt (mg/g) are the biosorption capacity at equilibrium and at any time t (min) respectively. The k_1 values which is rate constant of pseudo-first-order adsorption are obtained from slopes of linear plots log (qe-qt) versus time [16]. The pseudo-second order kinetic equation is given as follows;

$$\frac{t}{qt} = \frac{1}{k_2 q^2} + \frac{t}{qe} \quad (12)$$

Where K_2 is the pseudo second-order biosorption rate coefficient (g/mg min), q_e and q_t remains the biosorption capacity at equilibrium (mg/g) at time t (mins) respectively [16].

2.2.9 Thermodynamic parameters

The effect of temperature on the biosorption process of Cr and Ni using groundnut shell activated carbon was studied at different temperatures so as to obtain the thermodynamic parameters change in Gibb's free energy (ΔG°), enthalpy (ΔH°) and entropy (ΔS°) by using the following equations.

$$k_d = \frac{q_e}{C_e} \quad (13)$$

$$\Delta G^o = -RT\ln K_d \quad (14)$$

$$\Delta G^o = \Delta H^o - T\Delta S^o \quad (15)$$

Bringing the free energy equation (13) and (14) together will produce equation (15);

$$\ln k_d = \frac{\Delta S^0}{R} - \frac{\Delta H^0}{RT} \quad (16)$$

Where, q_e = amount of heavy metals biosorbed on biosorbent at equilibrium (mgg^{-1}), Ce =concentration of heavy metals in solution at equilibrium ($mg\ L^{-1}$), and k_d =the distribution coefficient, ΔG° (kJ/mol) =Gibbs free energy, ΔS° (kJ/molK) = Entropy change, ΔH° (kJ/mol) = Enthalpy change.

2.2.10 Experimental modelling and process optimization

The Response Surface Methodology (RSM) modelling technique was used to model the process and their performance and predictive capacity of the response (biosorption efficiency) on removal of heavy metals from oil mill industrial wastewater was examined. The experimental modeling was performed using the design expert (v12.0) software in order to determine the optimum combination and study the effect of process parameters on biosorption of heavy metals.

3. DISCUSSION OF RESULTS

3.1 Proximate Analysis

Proximate analysis for the raw groundnut shell is presented in Table 1

Table 1 Shows proximate analysis for groundnut shell

Description	% Moisture	% Ash	% Volatile Matter	%Fixed Carbon
Groundnut shell	4.92	4.56	76.79	13.73

Volatile matter content signifies the organic compound and ash content shows the amount of inorganic substituent in the activated carbon. Fixed carbon measures non-volatile carbon remaining in the sample after combustion. Fletcher et al [11] reported that materials with low moisture and ash content are a sign of good carbon material that is desirable for biosorption analysis.

3.2 Activated Carbon Percentage Yield

3.2.3 Groundnut shell activated carbon percentage yield

The percentage yield of groundnut shell activated carbon was obtained to be 37.53 % which indicated a significant carbon content in the groundnut shell, this shows how much of the raw material was converted into the final product.

3.3 Characterization

3.3.1 Fourier-transform infrared spectroscopy (FT-IR) analysis

Figure 1 shows the functional groups of groundnut shell and groundnut shell activated carbon, the result shows a common trend of the peaks and bands for the two samples, peaks observed at 3,652 cm^{-1} and 3,447 cm^{-1} were attributed to (OH) hydroxyl group while the bands seen at 2,885 cm^{-1} and 2762 cm^{-1} were attributed to R-COOH carboxyl acids. The peaks at 1,994 and 1,893 cm^{-1} indicated C-H bending vibrations and the bands at 1,684 cm^{-1} indicated strong C=O carbonyl groups. The peaks corresponding to phosphate group (PO_4^{2-}) was observed at 1420 cm^{-1} for GS-AC spectra, these bands shows the presence of phosphorus and oxygen compounds in the sample, biosorption of heavy metals in these region is commonly seen in carbon activated with H_3PO_4. The bands at 790cm^{-1} were ascribed to strong C-H bending vibrations. The FTIR result shows that the samples of groundnut shell activated carbons and are rich in essential surface functional group which in turn helps in biosorption of heavy metals.

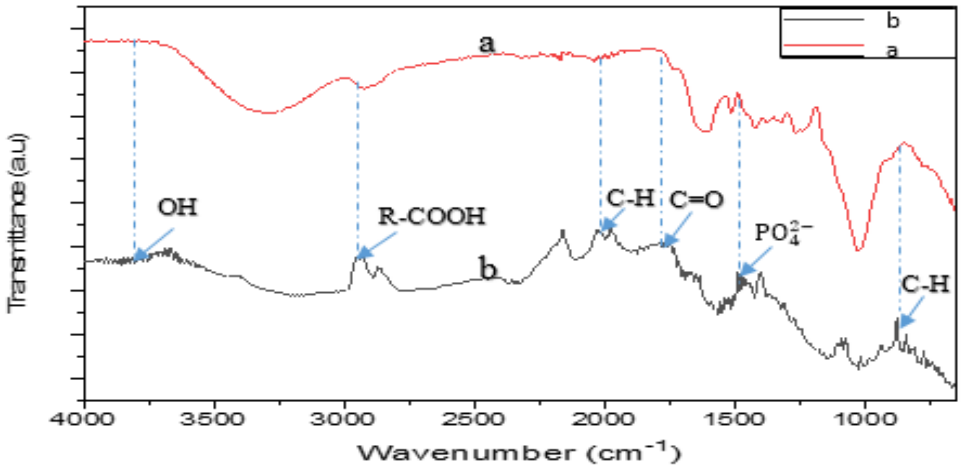

a Groundnut shell (GS) b Groundnut shell activated carbon (GS-AC)

Figure 1: FT-IR spectra of groundnut shell and groundnut shell activated carbon

3.3.2 Scanning electron microscopy, energy dispersive x-ray (SEM-EDX) analysis

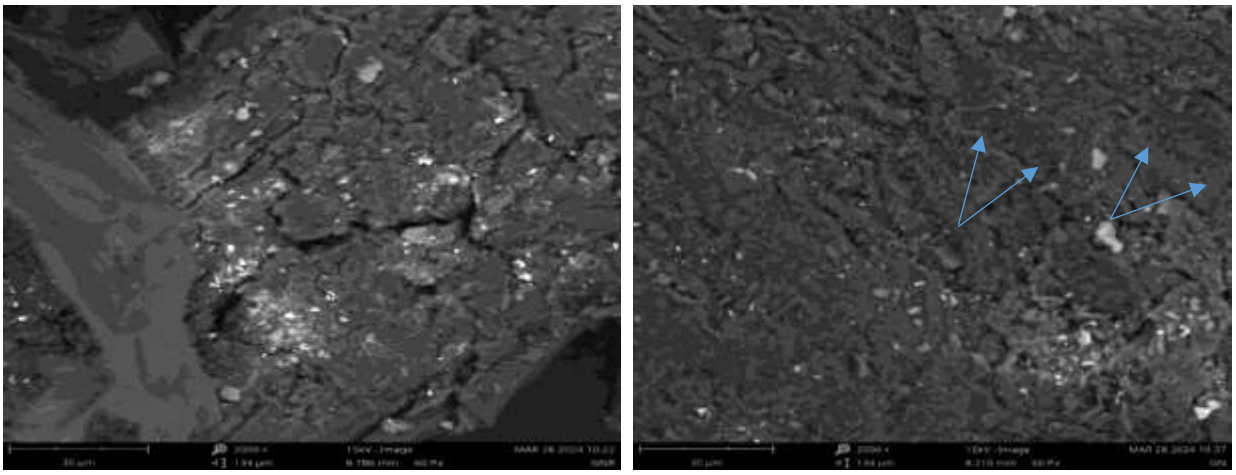

(a) (b)

Figure 2 (a) SEM images for groundnut shell GS and 2 (b) groundnut shell activated carbon GS-AC.

SEM analysis was conducted to observe the surface morphology of groundnut shell (GS) and groundnut shell activated carbon (GS-AC). These images were used to verify the possible changes in morphological features of the sample of raw material and activated carbon.

As shown in figure 2(b) the surfaces of groundnut shell activated carbon GS-AC were coarse and rough, with a dense fibrous and complex pore structures having uneven crevices with varying dimensions, pore structures were visible in the activated carbon which leads to surface area rise of the biosorbent and porous structure. These are micropores and mesopores which are potential sites for biosorption of heavy metals.

Table 2: EDX showing the elemental compositions of the groundnut shell activated carbon

Element Number	Element Symbol	Element Name	Atomic Concentration	Weight Concentration
6	C	Carbon	67.81	61.98
8	O	Oxygen	28.65	32.83
7	N	Nitrogen	2.68	2.85
15	P	Phosphorus	0.14	0.32
47	Ag	Silver	0.04	0.31
30	Zn	Zinc	0.06	0.28
14	Si	Silicon	0.13	0.27
11	Na	Sodium	0.12	0.20
13	Al	Aluminium	0.09	0.19
12	Mg	Magnesium	0.08	0.14
22	Ti	Titanium	0.04	0.14
26	Fe	Iron	0.03	0.12
16	S	Sulfur	0.05	0.12
19	K	Potassium	0.03	0.09
17	Cl	Chlorine	0.03	0.09
20	Ca	Calcium	0.02	0.07

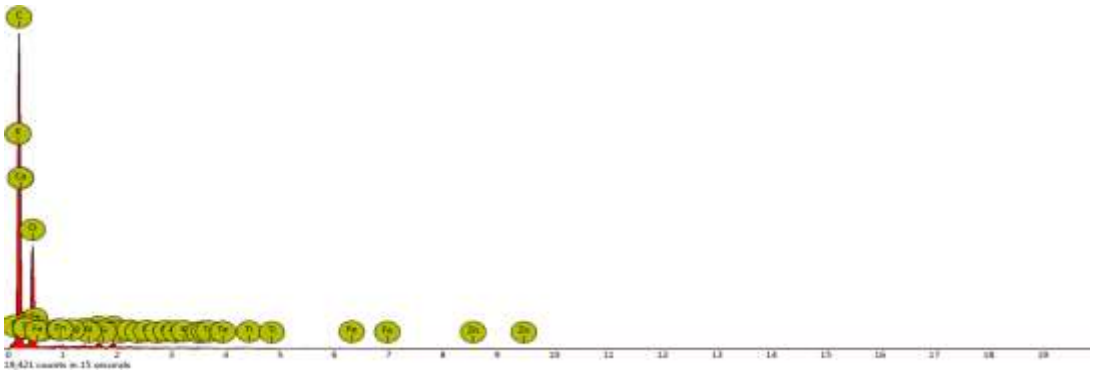

Figure 3: The EDX Image of the of the groundnut shell activated carbon

Table 2 shows the elemental composition of groundnut shell activated carbon (GS-AC) while Figure 3 shows the EDX analysis of groundnut shell activated carbon, it was noticed that the peaks of carbon and oxygen are the two major prominent peaks among other elements which confirms the carbon to oxygen ratio which corresponds to carbon (67.81%) and oxygen (28.65%) in the groundnut shell activated carbon. The prominent peaks of carbon (C) and oxygen (O) were observed with few subsided peaks of Titanium (Ti), nitrogen (N), zinc (Zn), phosphorus (P) and iron (Fe) which reveals that the groundnut shell activated carbon is evenly distributed with traces of carbon and oxygen due to carbonization, also reported in the works of [17].

3.3.3 Surface area (S_{BET}) analysis

Table 3 shows the surface area of groundnut shell activated carbon (GS-AC) as S_{BET} 689.41 m^2/g, the average pore size of 2.647nm and pore volume of 0.2437 cm^3/g.

Nguyen *et al* reported that activated carbons are categorized based on their average pore sizes as micropores (pore size < 2 nm), while mesopores if (2 nm< pore size <50 nm) and macroporous materials have pore size of greater than 50 nm [18].

This study, also shows using H_3PO_4 as an activating agent, the surface area of groundnut shell activated carbon (GS-AC) was S_{BET} 689.41 m^2/g. The values of groundnut shell activated carbon GS-AC S_{BET} surface area is in agreement with the discovery of other research work. [17], also reported GS-AC S_{BET} 533.94 m^2/g with an average pore size of 3 nm and pore volume of 0.475 cm^3/g. [19] also reported using H_3PO_4 as an activator on activated carbon increased the pore diameter and enlarged the pore volume and surface area.

In this work GS-AC activated carbon produced has a high surface area, micropore, mesopore percentage and pore volume could be ascribed to the lignocellulosic component (lignin, cellulose, and hemicellulose) of the raw material and effect of H_3PO_4 chemical activation. The prepared carbon was seen as naturally mesoporous with the pore size diameter between 2 and 50 nm.

Table 3: Surface area, pore size and pore volume of groundnut shell activated carbon (GS-AC)

Materials	S_{BET} (m^2/g)	Pore Size (nm)	Pore Volume (cm^3/g)
Groundnut shell activated carbon	689.41	2.647	0.2437

3.4. Response Surface Methodology

3.4.1. Modelling

The Response Surface Methodology (RSM) modelling was done according to Table 4, 5 and 7. Using the Central Composite Design (CCD) of design expert software with ranges of parameters for each process factors considered as shown in Table 4. The generated data from design of experiment (DOE) were analyzed and optimized using the design expert software and then interpreted. The experimental values were close to the predicted values for Response Surface Methodology (RSM) for a specific experimental run.

Table 4: Experimental design matrix for biosorption efficiency of Cr and Ni removal with the RSM modelling techniques.

Runs	Factor 1 A: Adsorbent dosage (g)	Factor 2 B: Temperature (^oC)	Factor 3 C: Time (hr)	Biosorption Efficiency %			
				Experimental		RSM Predicted	
				Cr	Ni	Cr	Ni
1	1.6	40	1.5	95.9	90.9	95.96	90.7
2	1.6	40	1.5	95.3	90.7	95.48	90.6
3	1.6	65.2	1.5	88.8	81.0	87.69	81.3
4	1.6	40	1.5	95.39	90.4	95.52	90.6
5	3.95	40	1.5	91.6	80.3	91.06	80.5
6	0.2	55	2	92.2	93.1	92.72	93.2
7	0.2	25	2	86.5	84.9	86.40	85.1
8	3	55	1	82.6	80.8	82.96	80.6
9	1.6	14.8	1.5	80.9	70.8	81.10	70.9
10	1.6	40	1.5	94.72	90.8	94.69	90.6
11	1.6	40	0.66	90.4	80.9	89.51	80.7
12	1.6	40	1.5	95.0	90.3	94.8	90.5
13	3	25	2	92.8	66.1	92.16	66.2
14	1.6	40	2.34	85.7	82.5	85.62	82.1
15	1.6	40	1.5	94.92	90.5	95.13	90.6
16	0.2	25	1	80.1	82.4	79.97	82.1
17	3	55	2	74.4	78.8	75.29	78.5
18	3	25	1	93.6	81.3	93.85	81.6
19	0.02	40	1.5	68.3	60.2	68.1	60.1
20	0.2	55	1	96.3	93.8	96.57	93.85

In this work a second-order polynomial that is, a quadratic model was also developed based on the relationship between independent variable and the responses as shown in Table 4. The Adequacy of the model established was checked by analysis of variance (ANOVA), f-test, significance level of the modelled factors and coefficient of determination (R^2). Graphs of response surface with contour were developed to analyze the connection between independent and dependent variables. To optimize the independent variable numerical optimization technique was also carried out.

i. **Analysis of variance (ANOVA) on biosorption efficiency for chromium removal**: Table 5 shows the ANOVA table for the level of significance of each of the modelled factors on biosorption efficiency for Cr removal. The result from Table 5 shows that the individual parameter (A-adsorbent dosage, B-temperature and C-time) has an important level of influence in determining the biosorption efficiency as seen from the F-value of 28.14, 90.2 and 36.32 respectively likewise the interactive effect of these process parameters (AB, AC, BC, B^2, C^2) shows significant level in the biosorption process as compared to A^2 which is not significant with F-value of 2.40 for Cr removal.
Table 6 shows the fit statistics with value of R^2= 0.9939 for Cr removal which is near unity signifying limited errors from the modeling. Graph of predicted vs actual values from Figure 4 also confirmed that no much error was observed from the modelling. For a good fit of a model Aklilu [20] recommend that R^2 value should be at least 0.80 [20]. The value of the adjusted R^2 for biosorption efficiency was 0.9884, which certify that the model was very important, suggesting good agreement between the experimental and predicted values of the response variables. Owolabi *et al* [21] suggested that adjusted R^2 and predicted R^2 should be within 20% to be in good concession [21].

ii. **Modelled equation of biosorption efficiency for Chromium (Cr) removal:**
Biosorption efficiency = 0.156170 + 18.26675*A + 2.35816*B + 48.01553*C – 0.318309*A*B + 2.77419*A*C – 0.257489*B*C – 0.621831* A^2 – 0.018130* B^2 – 11.86546* C^2 (13)
Where A=Adsorbent dosage, B=Temperature and C=Time

Equation (13) shows the relationship between biosorption efficiency and the operating parameters effect for chromium removal. Single-factors reveal the effect of a specific factor, while mixed quantities of two factors shows the effect of

interaction between two variables. The positive signs in the model reveal the synergetic effect of factors, while the negative sign shows the antagonistic effects.

Table 5: ANOVA for quadratic model for Cr removal

Source	Sum of Squares	Df	Mean Square	F-Value	P-Value	
Model	861.67	9	140.19	80.43	< 0.0001	Significant
A-Adsorbent dosage	6.67	1	6.67	28.14	0.0342	
B-Temperature	4.69	1	4.69	90.23	<0.0001	
C-Time	18.94	1	18.94	36.32	0.0085	
AB	377.66	1	377.66	72.48	<0.0001	
AC	32.36	1	32.36	6.21	0.00319	
BC	47.25	1	47.25	9.07	0.0013	
A^2	12.50	1	12.50	2.40	0.0023	
B^2	278.19	1	278.19	53.39	< 0.0001	
C^2	164.87	1	164.87	31.64	0.0002	
Residual	6.11	10	5.21			
Lack of Fit	5.80	5	1.36	2.04	0.0012	not significant
Pure Error	0.3101	5	0.0620			
Cor Total	867.78	19				

Table 6: Fit statistics from the ANOVA for Cr removal

Std. Dev.	2.28	**R^2**	0.9939
Mean	85.62	**Adjusted R^2**	0.9884
C.V. %	2.67	**Predicted R^2**	0.9448
		Adeq Precision	59.7325

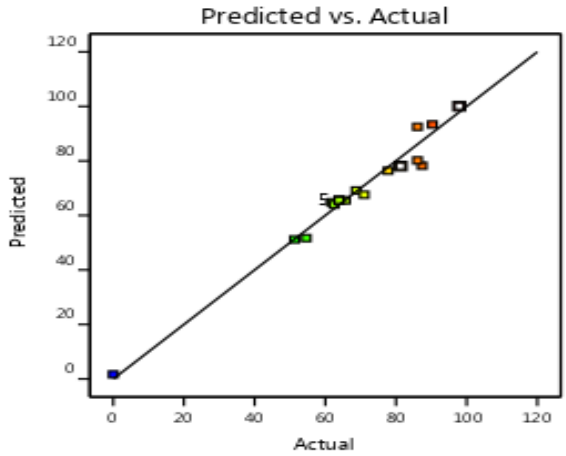

Figure 4: Predicted values versus actual values of biosorption efficiency for Cr removal.

iii. Analysis of variance (ANOVA) on biosorption efficiency for Nickel removal: Table 7 shows the ANOVA table for the level of significance of each of the modelled factors on biosorption efficiency for Ni removal. The result from Table 7 shows that the individual parameter (A-adsorbent dosage, B-temperature and C-time) has an important level of influence in determining the biosorption efficiency as seen from the F-value of 42.91, 24.13 and 20.01 respectively likewise the interactive effect of these process parameters (AB, AC, B^2, C^2) shows significant level in the biosorption process as compared to BC, A^2 which is not significant with F-value of 2.228 and 3.18 for Ni removal.

Table 8 shows the fit statistics with value of R^2= 0.9891 for Ni removal which is near unity signifying limited errors from the modeling. Graph of predicted vs actual values from Figure 5 also confirmed that no much error was observed from the modelling. For a good fit of a model Aklilu [20] recommend that R^2 value should be at least 0.80 [20]. The value of the adjusted R^2 for biosorption efficiency was 0.9792, which certify that the model was very important, suggesting good agreement between the experimental and predicted values of the response variables. Owolabi *et al* [21] suggested that adjusted R^2 and predicted R^2 should be within 20% to be in good concession [21].

iv. Modelled equation of biosorption efficiency for Nickel (Ni) removal

Biosorption efficiency = 0.352215 + 3.67063*A + 2.57468*B + 52.69903*C – 0.076508*A*B – 2.91564*A*C + 0.054038*B*C – 0.299490* A^2 – 0.028365* B^2 – 17.49202* C^2 (14)

Where A=Adsorbent dosage, B=Temperature and C=Time

Equation (14) shows the relationship between biosorption efficiency and the operating parameters for nickel removal. Single-factors reveals the effect of a specific factor, while mixed quantities of two factors shows the effect of interaction between two variables. The positive signs in the model reveals the synergetic effect of factors, while the negative sign shows the antagonistic effects.

Table 7: ANOVA for quadratic model for Ni removal

Source	Sum of Squares	Df	Mean Square	F-Value	P-Value	
Model	945.25	9	416.01	100.63	< 0.0001	Significant
A-Adsorbent dosage	390.68	1	390.68	42.91	< 0.0001	
B-Temperature	219.69	1	219.69	24.13	0.0006	
C-Time	18.31	1	18.31	20.01	0.0018	
AB	21.82	1	21.82	24.05	0.0015	
AC	35.74	1	35.74	39.30	0.0004	
BC	2.08	1	2.08	2.2286	0.0642	
A^2	2.90	1	2.90	3.3185	0.0584	
B^2	680.91	1	680.91	74.79	< 0.0001	
C^2	358.31	1	358.31	39.36	< 0.0001	
Residual	8.1433	10	6.10			
Lack of Fit	8.01	5	8.18	6.81	0.0023	not significant
Pure Error	0.1333	5	0.0267			
Cor Total	953.3933	19				

Table 8: Fit statistics from the ANOVA for Ni removal

Std. Dev.	3.02	**R^2**	0.9891
Mean	81.20	**Adjusted R^2**	0.9792
C.V. %	3.72	**Predicted R^2**	0.8860
		Adeq Precision	44.9450

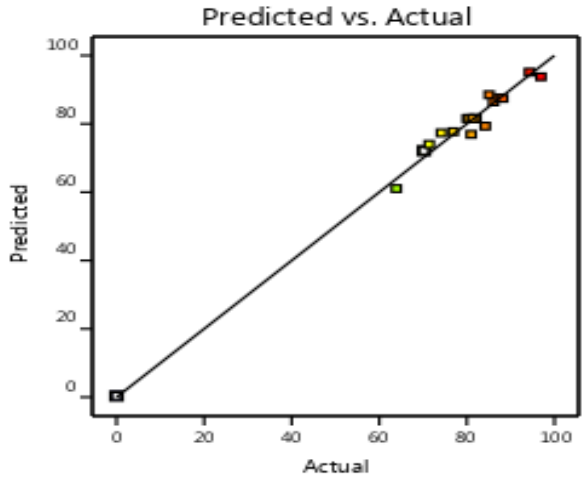

Figure 5: Predicted values versus actual values of biosorption efficiency for Ni removal.

3.4.2 Optimization

Process optimization was done for the process factors (Adsorbent dosage, time and Temperature) and optimal conditions for maximum biosorption efficiency of heavy metals are summarized in Table 9. Table 10 shows the Response Surface Methodology (RSM) Optimal process conditions for biosorption efficiency are 0.4 g for adsorbent dosage, 42.02 ^{o}C for temperature and 1.1 hr for biosorption time, and shows the percentage biosorption for RSM predicted and the validated experimental biosorption efficiency for Cr and Ni removal, this suggest accuracy of the model developed and a good agreement between the predicted and experimental values of the response variables. Figure 6(a) and 6(b) shows the Three-dimensional (3D) surface plot after optimization for the combined effects of adsorbent dosage, time and temperature biosorption efficiency at the optimal RSM values for Cr and Ni removal. Figure 6(a) and 6(b) indicates that biosorption efficiency increases with temperature increase above 40 °C and decreases with increasing adsorbent dosage.

Table 9: Process factors for optimization and optimal responses for Cr and Ni removal

Factors	Cr	Optimal Responses	Ni	Optimal Responses
Adsorbent dosage (grams)	Range	0.40	Range	0.4002
Temperature (^{o}C)	Range	42.02	Range	42.016
Time(hrs)	Range	1.102	Range	1.10
Biosorption Efficiency (%)	Maximum	97.0791	Maximum	94.7831
Desirability	1.0		1.0	

Table 10: Response Surface Methodology (RSM) optimal conditions and biosorption efficiency

Adsorbent dosage (g)	Temperature (^{o}C)	Time (hr)	Biosorption %			
			RSM predicted		Experimental	
			Cr	Ni	Cr	Ni
0.40	42.02	1.1	96.57	93.85	97.08	94.78

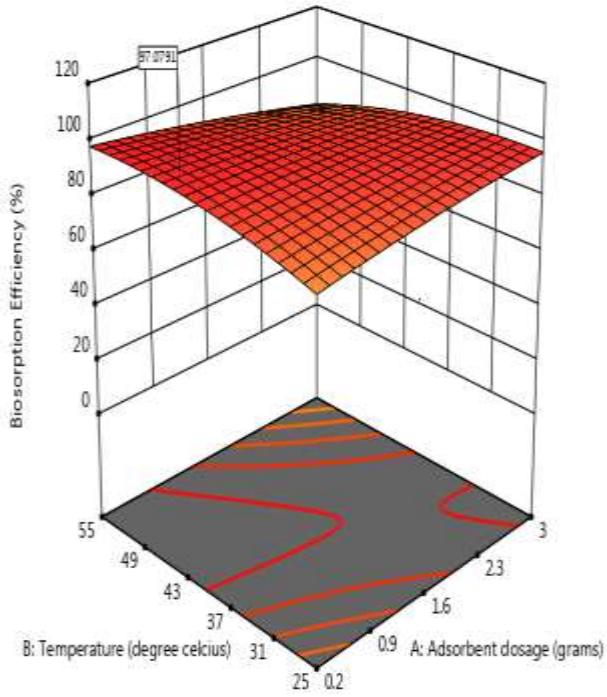

Figure 6a

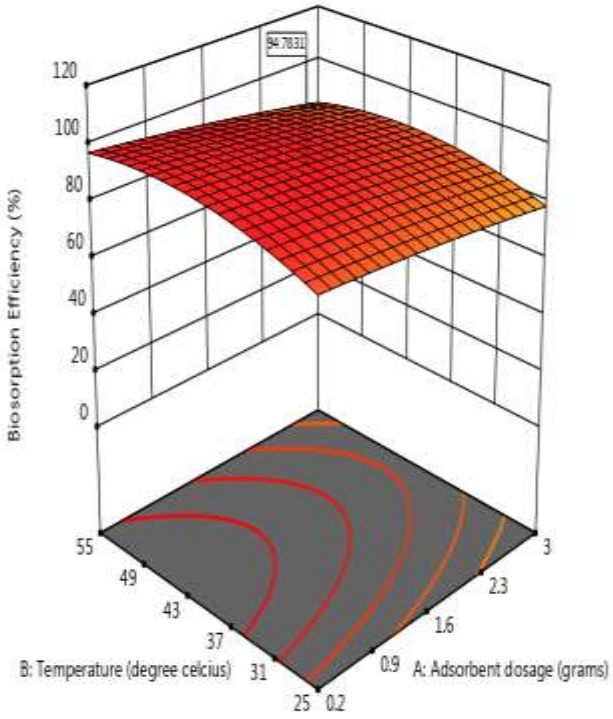

Figure 6b

Figure 6(a) and 6(b): 3-dimensional surface plot for effect of temperature and adsorbent dosage on biosorption efficiency at constant time 1.1 hr for Cr and Ni removal

3.5 Biosorption Isotherm Studies

3.5.1 Langmuir and Freundlich biosorption isotherm for Cr and Ni removal

Figure 7 shows the plot of Ce/qe vs Ce which fitted well for Cr removal and gave a linear plot with correlation coefficient of R^2=0.9983 and a root mean square error (RMSE=0.146). The slope and intercept of the line was used to calculate other Langmuir isotherm parameters which include q_m= 0.865 mg/g, K_L= 0.650 L/mg, R_L= 0.699. This result shows that the adsorption value ($q_{m=}$ 0.865 mg/g) as well as Langmuir constant K_L= 0.650 L/mg values shows maximum biosorption of Cr at the surface of the biosorbent with the Langmuir isotherm model as compared with the Freundlich isotherm model.

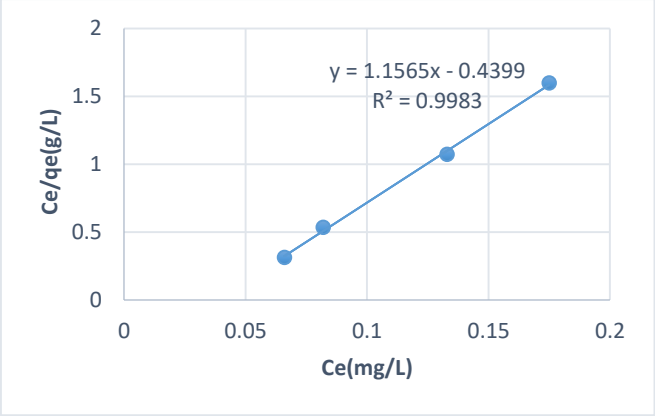

Figure 7: Langmuir biosorption isotherm plot showing Ce/qe vs Ce for Cr removal

Figure 8 shows a plot of ln qe vs ln Ce for Cr removal gave a line with R^2 = 0.9539 and RMSE=0.468. The Freundlich parameters was also evaluated from the slope and intercept of the line as thus; K_F=1.8813 mg/g and n=2.985

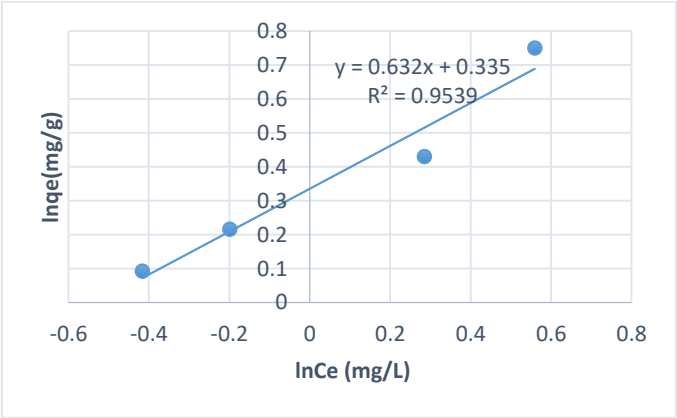

Figure 8: Freundlich biosorption isotherm plot showing ln qe vs ln Ce for Cr removal

Figure 9 shows the plot of Ce/qe vs Ce fitted well for Ni removal and gave a linear plot with correlation coefficient of R^2=0.9973 and a root mean square error (RMSE=0.203). The slope and intercept of the graph was used to calculate other Langmuir isotherm parameters which include q_m= 0.299 mg/g, K_L= 0.425 L/mg, R_L= 0.880. This result shows that the adsorption value ($q_{m=}$ 0.299 mg/g) as well as the Langmuir constant K_L= 0.425 L/mg values shows maximum biosorption of Ni on the surface of the biosorbent with the Langmuir isotherm model as compared with Freundlich isotherm model.

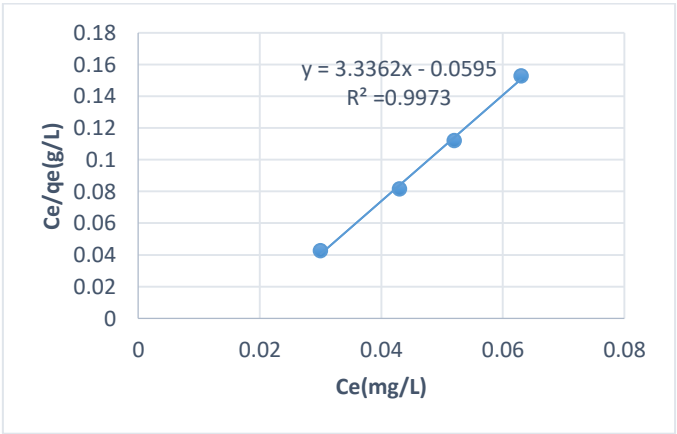

Figure 9: Langmuir biosorption isotherm plot showing Ce/qe vs Ce for Ni removal

Figure 10 shows a plot of ln qe vs ln Ce for Ni removal gave a line with R^2 = 0.9296 and RMSE=0.658. The Freundlich parameters was also evaluated from the slope and intercept of the line as thus; K_F=1.2484 mg/g and n=1.9976

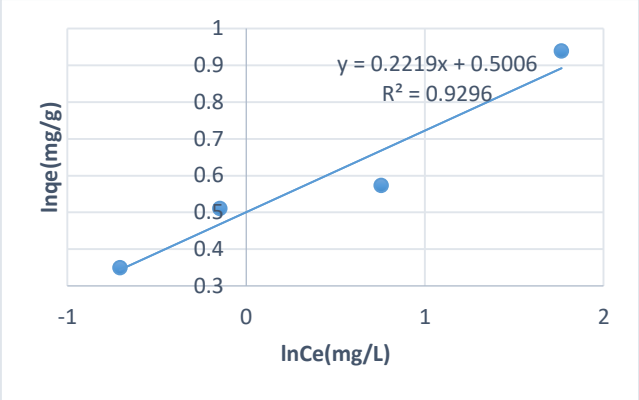

Figure 10: Freundlich biosorption isotherm plot showing ln qe vs ln Ce for Ni removal

Table 11: Biosorption isotherms for Cr and Ni removal

Isotherms	Metals	Model	Linear Form	Plots	Kinetic Parameters
Langmuir	Cr	$q_e = \frac{q_m KLC_e}{1 + KLC_e}$	$\frac{C_e}{q_e} = \frac{1}{q_m KL} + \frac{C_e}{q_m}$	Ce/qe vs Ce	q_m=0.865mg/g K_L=0.650L/mg, R_L=0.699 R^2=0.9983
Freundlich	Cr	$q_e = K_F C_e^{\frac{1}{n}}$	$\ln q_e = \ln K_F + \frac{1}{n} \ln C_e$	ln qe vs ln Ce	K_F=1.8813mg/g n=2.985 R^2= 0.9539
Langmuir	Ni	$q_e = \frac{q_m KLC_e}{1 + KLC_e}$	$\frac{C_e}{q_e} = \frac{1}{q_m KL} + \frac{C_e}{q_m}$	Ce/qe vs Ce	q_m=0.299mg/g K_L=0.425 L/mg R_L=0.880. R^2=0.9973
Freundlich	Ni	$q_e = K_F C_e^{\frac{1}{n}}$	$\ln q_e = \ln K_F + \frac{1}{n} \ln C_e$	ln qe vs ln Ce	K_F=1.2484mg/g n=1.9976 R^2= 0.9296

3.6 Kinetic Study

The Lagergren Pseudo-first order model as shown from Figure 11 and 13 was used to describe the biosorption kinectics of Cr and Ni. The results from the linear curve of the plot were analysed a correlation coefficient of R^2=0.9136 was obtained alongside the following parameters, k_1 (min^{-1}) = 0.1513 and q_e (mg/g) = 39.595

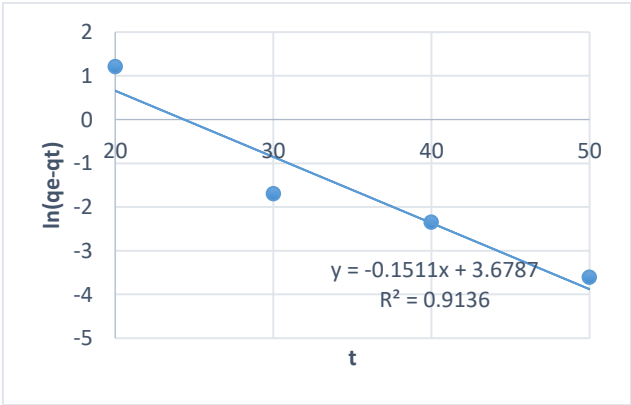

Figure 11: Plot of lagergren pseudo-first order for Cr removal

The pseudo-second-order kinetic model was also used to interpret the biosorption kinetics of Cr and Ni as shown below A linear plot of qt vs t as shown in Figure 12 gave a correlation coefficient of R^2 = 0.9976 and the following second order parameters were obtained; K_2 ($gmg^{-1}min^{-1}$) = 0.03146 and q_e (mg/g) = 12.59. The analyzed values of the correlation coefficient, R^2 for Pseudo-second order model was near to unity with the value higher making it fit well than the first order model. The calculated qe values were close with the experimental value (qe_{exp}= 12.53) for the pseudo second order model, revealing that biosorption of Cr followed a pseudo second order rate expression.

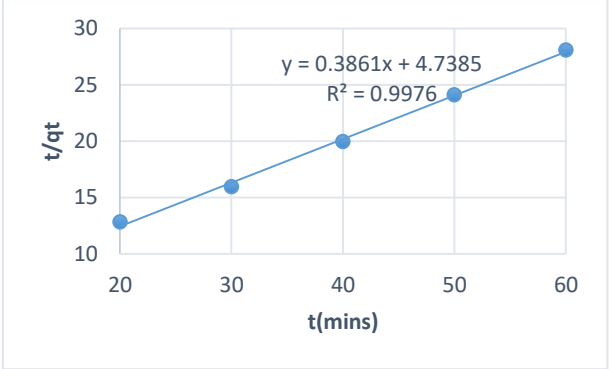

Figure 12: Plot of lagergren pseudo-second order for Cr removal.

The Lagergren Pseudo-first order model as shown from Figure 13 was used to describe the biosorption kinectics of Ni. The results from the linear curve of the plot were analysed a correlation coefficient of R^2=0.9206 was obtained alongside the following parameters, k_1 (min^{-1}) = 0.1062 and q_e (mg/g) = 14.169

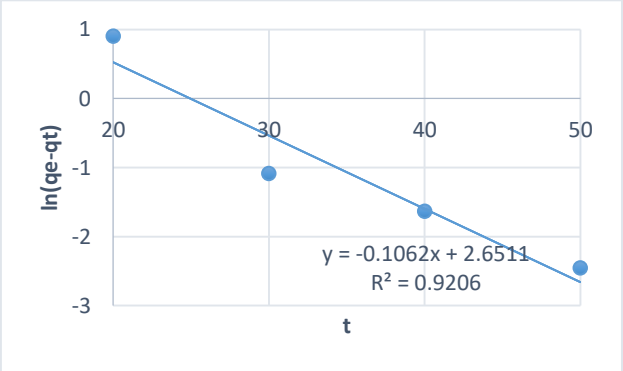

Figure 13: Plot of lagergren pseudo-first order for Ni removal

A linear plot of qt vs t as shown in Figure 15 gave an R^2 = 0.9936 and the following second order parameters were obtained for Ni removal; K_2 ($gmg^{-1}min^{-1}$) = 0.009211 and q_e (mg/g) = 6.039. The analyzed values of the correlation coefficient, R^2 for Pseudo-second order model was near to unity with value higher making it fit well than that of the first order model. The calculated qe values were close with the experimental value (qe_{exp}= 6.025) for the pseudo second order model, revealing that biosorption of Ni followed a pseudo second order rate expression

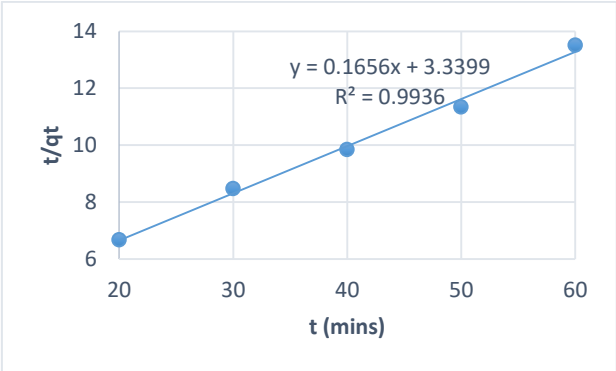

Figure 14 Plot of pseudo-second order for Ni removal

In conclusion, the (K_2=0.03146) values of pseudo second order kinetics is also found lower than that of the (K_1=0.1513) for the first order for Cr removal and the (K_2=0.00921) values of pseudo second order kinetics is also found lower than that of the (K_1=0.1062) for the first order for Ni removal as well as the closeness of the qe_{cal} and qe_{exp} suggest the adequacy of the pseudo second order reaction model for the biosorption reaction as compared to the pseudo first order for the removal of Cr and Ni. Biosorption rate constant decreases as the metal ion concentration increases validates that Cr and Ni uptake onto groundnut shell activated carbon gain equilibrium position quickly at a lower initial concentration. Similar trend was observed in the works of [17]

Table 12: Kinetic Study of Cr and Ni removal using groundnut shell activated carbon

Model	Metals	**Model Equation**	**Plots**	**Kinetic parameters**
Lagergren First-order	Cr	$\ln(qe-qt) = \ln qe - k_1 t$	ln(qe-qt) vs t	k_1 (min^{-1}) = 0.1513 q_e (mg/g) =39.595 R^2 = 0.9136
Pseudo second-order	Cr	$\frac{t}{qt} = \frac{1}{k_2 qe^2} + \frac{t}{qe}$	t/qt Vs t	k_2 ($gmg^{-1}min^{-1}$) = 0.03146 qe_{cal} (mg/g) =12.59 qe_{exp} =12.53 R^2 = 0.9976
Lagergren First-order	Ni	$\ln(qe-qt) = \ln qe - k_1 t$	ln(qe-qt) vs t	k_1 (min^{-1}) = 0.1062 q_e (mg/g) =14.1696 R^2 = 0.9206
Pseudo second-order	Ni	$\frac{t}{qt} = \frac{1}{k_2 qe^2} + \frac{t}{qe}$	t/qt Vs t	k_2 ($gmg^{-1}min^{-1}$) = 0.00921 qe_{cal} (mg/g) =6.039 qe_{exp} =6.025 R^2 = 0.9936

3.7 Thermodynamic Parameters

The enthalpy (ΔH^o) and entropy (ΔS^o) changes of the process was calculated from the slope and intercept of the line was obtained by plotting $\ln k_d$ versus 1/T from equation 16 as shown in Figure 15.

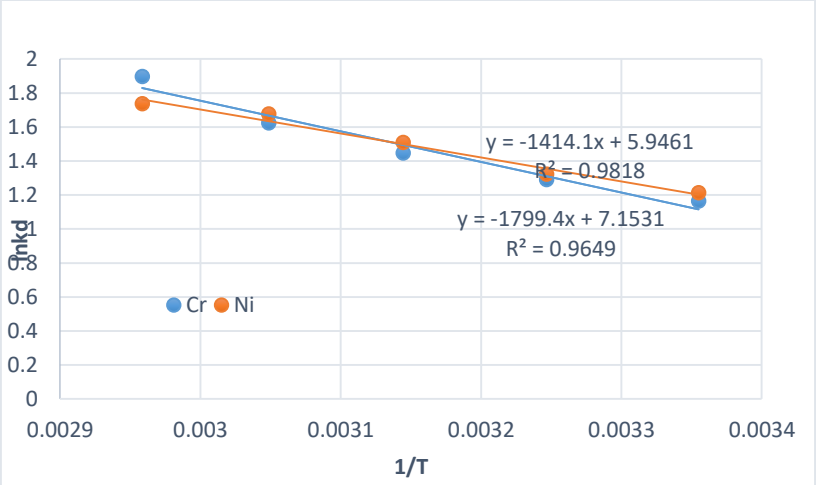

Figure 15: ln k_d Vs 1/T for Cr and Ni removal

Table 13: Thermodynamic parameters for Cr and Ni removal

Metals	**T(K)**	**ΔG° (kJ/mol)**	**ΔS° (kJ/molK)**	**ΔH° (kJ/mol)**
Cr	298	-2.76708	0.05947	14.9602
	308	-3.35674		
	318	-3.95146		
	328	-4.54619		
	338	-5.14082		
Ni	298	-2.96323	0.04944	11.7568
	308	-3.47074		
	318	-3.96512		
	328	-4.45958		
	338	-4.95392		

Table 13 shows the thermodynamic parameters (ΔG°, ΔS°, ΔH°) at different temperatures 25°C (298K), 35°C (308K), 45°C (318K), 55°C (328K) and 65°C (338K). The negative ΔG° values which is reducing as the temperature is increasing shows that the reaction was thermodynamically feasible and spontaneous while the positive enthalpy (ΔH°) and entropy (ΔS°) values confirmed the endothermic nature of the biosorption process and the increasing order at the solid-liquid boundary during the biosorption process respectively.

4. CONCLUSION

FT-IR characterization results shows the peaks of the expected functional groups in the FTIR spectra such as the OH, PO_4^{2-}, C-H, C=O, R-COOH carbonyl and carboxyl groups which are essential for heavy metals uptake during biosorption process. The surface area of groundnut shell activated carbon (GS-AC) was S_{BET} 689.41 m^2/g with an average pore size of 2.647nm and the pore volume of 0.2437 cm^3/g, the high surface area obtained was as a result of activation of carbon with H_3PO_4. SEM results showed increase of a good porous structure for groundnut shell activated carbon.

The optimum condition for removal of Cr and Ni was adsorbent dosage 0.40 g, contact time 1.10 hr and temperature 42.02 ^oC, which shows the maximum biosorption efficiency of 97.08% for Cr removal and 94.78% for Ni removal. The high biosorption efficiency of the groundnut shell activated carbon with its advantages such as abundance nature, environmental-friendly nature, reusability and low cost makes it a better alternative to be used than other commercial adsorbents for the uptake of the heavy metals.

The obtained data from the two isotherm studies proved that Langmuir best described the adsorption process on both Cr and Ni removal. The Langmuir isotherm with an R^2 value of 0.9983 and 0.9973 for Cr and Ni removal fits well with the experimental data and is higher than that of Freundlich isotherms which may be due to homogenous distribution on the active sites of the biosorbents. Kinetics data were best fitted by the pseudo-second order model with an R^2 value of 0.9976 and 9936 for Cr and Ni removal, while thermodynamics parameters obtained as seen from the positive enthalpy ($\Delta H°$=14.96021), entropy ($\Delta S°$=0.05947) and enthalpy ($\Delta H°$=11.7568), entropy ($\Delta S°$=0.04944) for Cr and Ni removal respectively and negative $\Delta G°$ values which is reducing as the temperature is increasing for Cr and Ni removal shows that the biosorption process was endothermic and spontaneous.

REFERENCES

[1] Kanamarlapudi S. L. R. K., Chintalpudi V. K. & Muddada S., (2018). Application of Biosorption for Removal of Heavy Metals from Wastewater. *IntechOpen*, 4, 70-116. DOI: 10.5772/intechopen.77315.

[2] Ingrao C., Strippoli R., Lagioia G. & Huisingh D. (2023). Water scarcity in agriculture: An overview of causes, impacts and approaches for reducing the risks. *Heliyon*, 9(8): e18507. doi:10.1016/j.heliyon.2023.e18507

[3] Tripathi A. & Ranjan M. R. (2015). Heavy Metal Removal from Wastewater Using Low Cost Adsorbents. *J Bioremed Biodeg.*, 6, 3-15. doi:10.4172/2155-6199.1000315

[4] Duc P. A., Dharanipriya P., Velmurugan B. K. and Shanmugavadivu M. (2019). Groundnut shell –a beneficial bio-waste. *Biocatalysis and Agricultural Biotechnology*. 20:1878-8181, https://doi.org/10.1016/j.bcab.2019.101206

[5] Dika J. (2015) Production of activated carbon from combined precursor raw materials (coconut shell and sawdust). 2015;8:9-12

[6] Olawale A. S., Ajayi O. A., Olakunle M. S., Ityokumbul M.T. & Adefila S. S. (2015). Preparation of phosphoric acid activated carbons from Canarium Schweinfurthii Nutshell and its role in methylene blue adsorption. *Journal of Chemical Engineering and Material Science*: 6(2), 9-14. DOI: 10.5897/JCEMS2015.0219

[7] Obayomi K.S., Bello J. O., Nnoruka J. S, Adediran A. A. & Olajide P.O. (2019). Development of low-cost bio-adsorbent from agricultural waste composite for Pb(II) and As(III) sorption from aqueous solution. *Cogent Engineering*, 6 (1), 72-74, https://doi.org/10.1080/23311916.2019.1687274

[8] Mwegoha W.J. & Lema M.W. (2016) Effectiveness of Activated Groundnut Shells to Remove Chromium from Tannery Wastewater. *International Journal of Environmental Monitoring and Protection*, 3(34),36-42

[9] Shruthi K.M. & Pavithra M.P. (2018) A Study on Utilization of Groundnut Shell as Biosorbent for Heavy Metals Removal. *International Journal of Engineering and Techniques*, 4(3):411-415.

[10] Vaddi D. R., Gurubelli T.R., Koutavarapu R., Lee D.Y. & Shim J. (2022). Bio-Stimulated Adsorption of Cr(VI) from Aqueous Solution by Groundnut Shell Activated Carbon @Al Embedded Material *Catalysts*, 12(3)290 290. https://doi.org/10.3390/catal12030290

[11] Fletcher A., Somorin T. & Aladeokin O. (2023) Production of High Surface Area Activated Carbon from Peanut Shell by Chemical Activation with Zinc Chloride: Optimization and Characterization. *Bionerg. Res*. 17, 467-478, https://doi.org/10.1007/s12155-023-10683-7

[12] Aydar, A. Y. (2018). Utilization of Response Surface Methodology in Optimization of Extraction of Plant Materials. *intech open science*, 10, 57-169, http://dx.doi.org/10.5772/intechopen.73690.

[13] Todorova K., Velkova Z., Stoytcheva M., Kirova G., Kostadinova S. & Gochev V., (2019). Novel composite biosorbent from Bacillus cereus for heavy metals removal from aqueous solutions. *Biotechnology and Botechnological Equipment*, 33(1), 730-738. DOI: 10.1080/13102818.2019.1610066

[14] Hammud H. H., El-Shaara A., Khamisb E. & Mansour E. (2014). Adsorption Studies of Lead by Enteromorpha Algae and its Silicates Bonded Material. *J. of Science*, 1, 1-26, DOI: 10.1155/2014/205459

[15] Uddin M. K., & Nasar A. (2020). Walnut shell powder as a low-cost adsorbent for methylene blue dye: isotherm, kinetics, thermodynamics, desorption and response surface methodology examinations. *Sci Rep* 10, 7983. DOI:10.1038/s41598-020-64745-3

[16] Elhadj, M., Samira, A., Mohamed,T., Djawad, F. & Asma, A. (2019). Removal of Basic Red 46 dye from aqueous solution by adsorption and photocatalysis: equilibrium, isotherms, kinetics, and thermodynamic studies. *Separation Science and Technology*, 1-17, https://doi.org/10.1080/01496395.2019.1577896.

[17] Eletta O. A. A., Tijani I. O. & Ighalo J. O. (2020). Adsorption of Pb(II) and Phenol from Wastewater Using Silver Nitrate Modified Activated Carbon from Groundnut (Arachis hypogaea L.) Shells. *The West Indian Journal of Engineering*, 43(1):26-35
[18] Nguyen H. D., Tran H. N., Chao H. P. & Lin C.C. (2019). Activated Carbons Derived from Teak Sawdust-Hydrochars for Effcient Removal of Methylene Blue, Copper, and Cadmium from Aqueous Solution. *Water*, 11, 2581, doi:10.3390/w11122581
[19] Kumari G., Soni B. & Karmee S. K. (2022). Synthesis of activated carbon from groundnut shell via chemical activation. *Journal of institution of Engineers (India)*, 103,15-22. DOI: 10.1007/s40034-020-00176-z
[20] Aklilu E. G. (2021). Artificial Neural Networks (ANNs) and Response Surface Methodology (RSM) Approach for Modeling and Optimization of pectin extraction from banana peel. 1-34, DOI:10.21203/rs.3.rs-102634/v1
[21] Owolabi, R. U., Usman, M. A., & Kehinde, A. J. (2018) Modelling and optimization of process variables for the solution polymerization of styrene using response surface methodology. *Journal of King Saud University - Engineering Sciences*, 30(1), 22–30. https://doi.org/10.1016/j.jksues.2015.12.005